Available online at www.sciencedirect.com
SCIENCE DIRECT®
Journal of Sound and Vibration 271 (2004) 1015–1038
JOURNAL OF SOUND AND VIBRATION
www.elsevier.com/locate/jsvi

Assessing the local stability of periodic motions for large multibody non-linear systems using proper orthogonal decomposition

G. Quaranta*, P. Mantegazza, P. Masarati

Dipartimento di Ingegneria Aerospaziale, Politecnico di Milano, via La Masa 34, 20156 Milano, Italy

Received 25 October 2002; accepted 14 March 2003

Abstract

The eigenvalues of the monodromy matrix, known as Floquet characteristic multipliers, are used to study the local stability of periodic motions of a non-linear system of differential-algebraic equations (DAE). When the size of the underlying system is large, the cost of computing the monodromy matrix and its eigenvalues may be too high. In addition, for non-minimal set equations, such as those of a DAE system, there is a certain number of spurious eigenvalues associated with the algebraic constraint equations, which are meaningless for the assessment of the stability of motions. An approach to extract the dominant eigenvalues of the transition matrix without explicitly computing it is presented. The selection of the eigenvalues is based on a *proper orthogonal decomposition* (POD), which extracts the minimal set of dominant local modes of the transient dynamics on an "energy" contents basis. To make the procedure applicable to both numerical and experimental tests, a unifying *experimental* philosophy is pursued for the analysis of complex multidisciplinary multibody models. Some applications are outlined, and comparisons with other techniques are presented to demonstrate the accuracy of the proposed procedure.

1. Introduction

Non-linear systems may possess a large variety of periodic motions, denominated limit cycles [1]. The local stability of these periodic orbits is assessed by computing the rate of attraction of their transients. These transients may be caused by imposing initial conditions which do not belong to the periodic orbit, or by perturbations of a steady state. Their behaviour can be investigated using Floquet's theory, originally developed for the analysis of the solution of linear

*Corresponding author. Tel.: +39-02-2399-8387; fax: +39-02-2399-8334.
E-mail address: quaranta@aero.polimi.it (G. Quaranta).

0022-460X/$ - see front matter © 2003 Elsevier Ltd. All rights reserved.
doi:10.1016/j.jsv.2003.03.004

ordinary differential equations with periodic coefficients [1–3]. The stability of the system can be inferred from the spectral radius of the monodromy matrix, which is the transition matrix that relates to two periodic solution state vectors separated by a time period. In classical applications of this method, the monodromy matrix is computed first; then its eigenvalues are evaluated. There are different methods to compute the monodromy matrix [4], but all of them are somewhat impractical to pursue for large numerical models, so this approach has been limited to systems with relatively few states.

Another convenient way to study the stability of periodic orbits is based on the construction of stroboscopic Poincaré maps. The idea is to reduce the study of continuous time systems to the analysis of associated discrete time systems. A Poincaré map can be constructed by defining a cross-section surface in the multidimensional phase space and measuring the transition of the system orbits through this surface [5]. In this way a local description of the transients is obtained. Of course, the periodic orbit in the phase space becomes a fixed point for the map. It can be shown that the eigenvalues of the Poincaré map are perfectly equivalent to the Floquet characteristic multipliers [5]. The stability condition, analogous to that of maps, states that the magnitude of the characteristic multipliers must be less than unity.

As a consequence of the increase in computer power, complex dynamical systems can be simulated using large-scale models. A typical example is the design of complex deformable aeroservomechanical systems that require sophisticated analyses, which are often conducted by means of general-purpose modelling codes based on a multibody/multidisciplinary methodology [6]. By means of these codes the designer can progress from simple rigid body models up to fully detailed ones, featuring accurate and fully non-linear description of constraints, deformable elements, servohydraulic circuits, aerodynamic forces and control system components [7]. These general-purpose modelling tools allow the investigation of a wide range of interactional phenomena between different subsystems. The size of the resulting model, pushed by the increasing demand for details in deformable bodies modelling, may soon become very large. The computation of the monodromy matrix and of its eigenvalues for these problems can be extremely demanding, both in terms of computational power and memory requirements.

An empirical method to reconstruct a local Jacobian of the Poincaré map from data obtained either by experiments or by simulations has been presented by Murphy et al. [8]. Despite being very interesting, this method, based on a least-squares identification of the Jacobian matrix, might become quickly unmanageable as the number of degrees-of-freedom used to represent the system increase.

Among the attempts to simplify the estimate of the stability boundaries for large-scale models, the work of Matthies and Nath [9] deserves a special mention; they conducted the stability analysis of an ordinary differential equation (ODE) system, resulting from the discretization of a partial differential equation (PDE) finite element model, by means of a coarser discretization, trying to reduce the effective system dimensions. Subramanian and Gaonkar proposed a parallel algorithm to speed up the research of the Floquet multipliers for large models, achieving only a limited overall computational time reduction [10]. A more computationally efficient approach has been proposed by Bauchau and Nikishkov [11,12]. It allows the evaluation of a limited number of eigenvalues of the monodromy matrix with the largest modulus using Arnoldi's iterative algorithm, without requiring the explicit computation of the matrix. Even though this method correctly assesses stability boundaries when the system is unstable, it may give misleading

information in evaluating the stability margin of periodic orbits since, for models based on DAE, spurious eigenvalues associated with algebraic constraints may arise. Furthermore, it cannot be applied to experimental data, as opposed to the approaches based on the explicit reconstruction of the Jacobian matrix.

The huge amount of information generated by numerical simulations, represented by the state vectors at each integration time step, must be synthesized to obtain few quantities of interest. In fact, providing a viable and efficient approach to condense the available data, while maintaining the capability of reliably finding the stability properties of periodic orbits, would make the technique presented in Ref. [8] feasible also for large systems, with the additional advantage of having at hand a unifying approach for numerical analyses and experimental tests. A powerful and elegant method of data analysis to obtain a low-dimensional approximate description of high-dimensional processes is the *proper orthogonal decomposition* (POD), also known as *Karhunen–Loéve decomposition*. There are many applications of POD. It has been extensively used in fluid mechanics, to study turbulent flows and to reduce the degrees-of-freedom of the numerical models [13], or in the reduction of complex viscous transonic aerodynamic fields inside turbomachinery [14]. Recently, it has been applied in dynamic studies of structural vibrations [15,16], and for damage detection [17]. Data analysis using POD is conducted to extract a set of basis functions, called proper orthogonal modes (POMs), from experimental data or from numerical simulations, to be subsequently used in a Galerkin projection yielding low-dimensional dynamical models. These functions are optimal, in the sense that fewer POD modes are needed to account for the same amount of "signal energy", compared to any other orthogonal basis [13]. Thus, the POMs are a minimal set of output signals that can be used to identify the dominant eigenvalues of the Jacobian matrix of the Poincaré map. After evaluating the multi-dimensional Poincaré maps associated with these signals, pieces of information regarding the dominant eigenvalues can be extracted by means of standard system identification procedures.

This paper is structured as follows: Section 2 briefly reviews the basics of the stability theory for periodic orbits and how it relates to Poincaré maps. Section 3 presents POD, and how it is applied to the extraction of the leading information regarding the stability of the motions under investigation. Section 4 summarizes all the steps required to apply the proposed method to assess the stability of motions. In Section 5 a brief introduction to DAE systems and how they are used to build multibody models is presented. By means of a simple example it is shown how spurious eigenvalues may arise. Finally, Section 6 presents two numerical examples to validate the proposed method and illustrate its accuracy. The first one addresses the stability of the classical problem of a beam subjected to a harmonic compressive follower force [18]. The second one shows the application of the presented technique to a multibody/multidisciplinary model, to study the ground resonance of a helicopter [19], a typical mechanical periodic instability.

2. Periodic orbits and their stability

Consider an autonomous N-dimensional dynamic system

$$\dot{\mathbf{x}} = \mathbf{f}(\mathbf{x}), \tag{1}$$

which possesses a periodic solution $\tilde{\mathbf{x}}(t) = \tilde{\mathbf{x}}(t+T)$, characterized in the phase space by the orbit γ. The stability of γ can be assessed by studying the way γ-neighbouring trajectories behave. By linearizing the differential equation about γ one obtains

$$\dot{\boldsymbol{\xi}} = \mathbf{Df}(\tilde{\mathbf{x}}(t))\boldsymbol{\xi}, \tag{2}$$

where $\mathbf{Df}(\tilde{\mathbf{x}}(t))$ is a periodic matrix. The monodromy matrix is the transition matrix computed on a period T, so it is defined as

$$\boldsymbol{\xi}(T) = \boldsymbol{\Phi}(T,0)\boldsymbol{\xi}(0). \tag{3}$$

Rearranging Eqs. (2) and (3), the transition matrix can be written as the solution of the following differential problem (see Seydel [4]):

$$\dot{\boldsymbol{\Phi}} = \mathbf{Df}(\tilde{\mathbf{x}}(t))\boldsymbol{\Phi}, \quad \boldsymbol{\Phi}(0,0) = \mathbf{I}. \tag{4}$$

Resorting to Floquet's theory [3,5], it can be shown how any fundamental solution matrix of this periodic system has the form

$$\boldsymbol{\Phi}(t,0) = \mathbf{Z}(t)\mathrm{e}^{\mathbf{B}t} \tag{5}$$

where $\mathbf{Z}$ is a T-periodic matrix. Since $\boldsymbol{\Phi}(0,0) = \mathbf{Z}(0) = \mathbf{I}$, the monodromy matrix is

$$\boldsymbol{\Phi}_T = \boldsymbol{\Phi}(T,0) = \mathrm{e}^{\mathbf{B}T}. \tag{6}$$

The eigenvalues of this matrix are the characteristic multipliers of the periodic orbit γ. The multiplier associated with perturbations along γ in the phase space is always equal to one, so the modules of the remaining $(N-1)$ multipliers orthogonal to γ determine the stability properties of the periodic orbit γ.

The study of the stability can also be accomplished by reducing the continuous system (1) to the $(N-1)$-dimensional associated discrete map $\mathbf{y}_{n+1} = \mathbf{F}(\mathbf{y}_n)$, called Poincaré map, where $\mathbf{y}$ is an $(N-1)$ state vector. This map is obtained by sampling the $(N-1)$ state variables, triggered by the orbit crossing an hyperplane transverse to the vector field $\mathbf{f}(\mathbf{x})$, usually called a *Poincaré section* (for further details see Ref. [5]). By definition a periodic orbit is one that revisits a point in the phase space once every period. So, the stability of a periodic orbit is reflected by the properties of the fixed points for the $(N-1)$-dimensional map. In fact, the eigenvalues of the linearized Poincaré map $\mathbf{DF}(\mathbf{y}_\gamma)$ correspond to the $(N-1)$ characteristic multipliers which determine the stability properties of the periodic orbit.

Non-autonomous periodically forced systems, $\dot{\mathbf{x}} = \mathbf{f}(\mathbf{x},t)$, may be treated in the same way by simply noting that they can be viewed as autonomous, at the expense of an increase of their dimension by one, i.e., including time as a state variable

$$\dot{\mathbf{x}} = \mathbf{f}(\mathbf{x},\theta),$$
$$\dot{\theta} = \omega,$$

where ω is the circular frequency of the periodic forcing signal. In this case the Poincaré section will be simply defined by any $\theta = \theta_0$, with $\theta_0 \in [0, 2\pi]$.

2.1. Evaluation of the monodromy matrix

The previous paragraph provides a sequence of steps required to estimate the stability of a periodic motion. First of all it is essential to evaluate the monodromy matrix $\mathbf{\Phi}_T$, or equivalently the Jacobian of the associated Poincaré map. As soon as this matrix is available, the stability of a periodic trajectory may be assessed by means of its eigenvalues. A fixed point for a discrete system is stable if and only if the spectral radius of the Jacobian, computed around the fixed point, is less or equal to unity. The classical method to generate the monodromy matrix is based on Eq. (4): integrating these N^2 differential equations for $0 \leqslant t \leqslant T$ yields the monodromy matrix but, since the Jacobian $\mathbf{Df}(\tilde{\mathbf{x}}(t))$ varies along the orbit γ and hence with time, it is necessary for the general non-linear case to integrate until $t = T$ the $(N + N^2)$-dimension initial value problem

$$\dot{\mathbf{x}} = \mathbf{f}(\mathbf{x}), \quad \mathbf{x}(0) = \tilde{\mathbf{x}}(0),$$
$$\dot{\mathbf{\Phi}} = \mathbf{Df}(\tilde{\mathbf{x}}(t))\mathbf{\Phi}, \quad \mathbf{\Phi}(0) = \mathbf{I}.$$

In case of linear systems only the last N^2 equations are required. Numerous methods have been proposed to reduce the overwhelming computational effort required to solve this problem. For an introductory description the reader is referred to the methods suggested by Seydel in Ref. [4]. In the linear case the problem can be simplified by using the method proposed by Friedmann et al. [20]. In any case, when the dimension N of the problem is large, the calculation of $\mathbf{\Phi}_T$ and all its eigenvalues may be too costly to be effectively used in most applications. Moreover, in practical analyses $\mathbf{\Phi}_T$ is seldom known analytically, so it must be obtained by a numerical linearization; as a consequence, the quality of its approximation must often be verified by means of repeated computations with different numerical parameters to assess the discretization errors. Finally, in any case most of the eigenvalues of $\mathbf{\Phi}_T$ do not give any useful insight for the investigation of stability problems. Thus, to simplify the stability analysis, it is necessary to find a method capable of estimating and selecting the dominant eigenvalues of $\mathbf{\Phi}_T$, which characterize the phenomenon under investigation, while reducing the computational burden as much as possible.

3. Extracting dominant transients from simulation

The approach followed here stems from the method proposed by Murphy et al. [8] and is strictly connected to the idea of numerical simulations viewed as "numerical experiments", whose results are analyzed by techniques that are suitable for experimental data as well. In essence, the monodromy matrix allows one to write the following expression:

$$\mathbf{x}^{(k+1)} = \mathbf{\Phi}_T \mathbf{x}^{(k)}, \tag{7}$$

where the index k is related to samples one period T apart. In the recursive equation written above the matrix $\mathbf{\Phi}_T$ must be evaluated starting from appropriate vectors $\mathbf{x}^{(k)}$, that are computed numerically by integrating Eq. (1) after applying a suitable perturbation. The perturbation must guarantee an adequate linearization while keeping the solution within the attraction basin of the periodic orbit under investigation. The different approaches for the determination of $\mathbf{\Phi}_T$ can be related to different interpretations of Eq. (7).

On one hand, it may be viewed as an auto-regressive (AR) discrete time model

$$\mathbf{X}^{(k+1)} = \mathbf{\Phi}_T \mathbf{X}^{(k)}, \tag{8}$$

where

$$\mathbf{X}^{(k+1)} = [\ldots \mathbf{x}^{(k+1)} \ \mathbf{x}^{(k)} \ldots],$$
$$\mathbf{X}^{(k)} = [\ldots \mathbf{x}^{(k)} \ \mathbf{x}^{(k-1)} \ldots],$$

which is a generalization of the least-squares linear fitting of the system response to an initial perturbation, observed either in experiments or simulations, to compute an approximation of the linearized Poincaré map presented in Ref. [8].

On the other hand, it can also be viewed as a power iteration, in which case the components ratio $\mathbf{x}^{(k+1)}/\mathbf{x}^{(k)}$ is known to converge to the largest eigenvalue of $\mathbf{\Phi}_T$, if the initial vector is not defective in the direction of the related eigenvector [21]. The power iteration (7), in principle, suffices to determine the stability boundaries. However, since the largest eigenvalue may not be well separated from neighbouring eigenvalues, the method must be extended to look the eigenvalues in the vicinity of the largest modulus one by using an iterative subspace method [22] where, at each step, the algorithm chooses the best initial conditions for Eq. (7).

Bauchau and Nikishkov propose an *implicit matrix method* [11] exploiting the properties of the Arnoldi's algorithm: a subspace method, which needs only a matrix-vector multiplication to extract the highest modulus eigenvalues of large and sparse matrices, and, at the same time, does not require the solution of the transpose problem, as other subspace methods for non-symmetric problems do. Therefore, the eigenvalues of the transition matrix $\mathbf{\Phi}(t, 0)$ can be obtained by performing a computation of the response after a certain time interval to an initial condition vector chosen by the algorithm. If a sufficiently small time interval is chosen, it is possible to evaluate the eigenvalues of the linearized system near an equilibrium condition. By choosing the period T as time interval, the eigenvalues of the monodromy matrix can be computed (if a periodic response exists). Even though this method gives the correct estimate of the stability boundary, it can be misleading in giving information about the stability margin of DAE systems. In fact, as it will be seen in Section 5, there are always unit modulus eigenvalues associated with the algebraic constraints.

A way must be devised to select a reduced set of signals synthesizing the information related to the dominant transient, to be able to apply any method for the evaluation of stability properties. These signals can be selected by resorting to a technique capable of extracting spatial coherence in an oscillating system, when the time history of its state variables is known from either numerical simulations or from the output of several sensors measured in real-life experiments. This method is represented by the POD used for the analysis of multi-dimensional data. It provides a way to find the best approximating subspace to a given set of data in a least-squares sense. The POD allows one to obtain a modal decomposition that is only data dependent and does not assume any prior knowledge of the system. Consequently, it perfectly fits the analysis needs of multidisciplinary models. A reduced order model of a dynamical system can be obtained by simply using a Galerkin projection procedure where the POD modes are used as basis functions. The same ideas can be applied here for the generation of a small subset of significant signals to be used for the identification of the leading eigenvalues characterizing system behaviour and stability. For the analysis of mechanical systems, it must be further noticed that these base POMs have an interesting interpretation, since they can be viewed as the result of a least-squares error optimization for a linear representation of the non-linear normal modes [15].

3.1. Computation of the proper orthogonal decomposition

Consider a system where all the N state variables are measured at n time steps. Their time averages are usually subtracted from the signals and data are arranged in a $(N \times n)$ matrix

$$\mathbf{X} = [\mathbf{x}^{(1)}, \mathbf{x}^{(2)}, \ldots, \mathbf{x}^{(n)}].$$

An approximation of the system dynamics is obtained by projecting the original N-dimensional state space onto an m-dimensional subspace $\mathscr{S}$. The main purpose of POD is to find a projection operator $\mathbf{Q}$ mapping $\mathbb{R}^N$ onto $\mathscr{S}$, which minimizes the Euclidean distance of the sampled points from the m-dimensional hyperplane

$$H(\mathbf{Q}) = \sum_{i=1}^{n} \|\mathbf{x}^{(i)} - \mathbf{Q}\mathbf{x}^{(i)}\|.$$

It can be shown (see Ref. [13]) that, given $\lambda_1 \geqslant \lambda_2 \geqslant \cdots \geqslant \lambda_n$, the eigenvalues of the data correlation matrix $\mathbf{R} = \mathbf{X}\mathbf{X}^{\mathrm{T}}$, the optimal m-dimensional projection operator is represented by the $(m \times N)$ matrix whose rows are the first m eigenvectors of $\mathbf{R}$. To obtain these eigenvectors, the singular value decomposition (SVD) of matrix $\mathbf{X}^{\mathrm{T}}$ can be computed:

$$\mathbf{X}^{\mathrm{T}} = \mathbf{U}\boldsymbol{\Sigma}\mathbf{V}^{\mathrm{T}},$$

where $\boldsymbol{\Sigma}$ is the diagonal matrix of the singular values σ_i, and the columns of $\mathbf{V}$ are the POMs. By sorting the singular values σ_i of $\mathbf{X}$ in a descending order, it can be shown that the matrix $\mathbf{X}_m^{\mathrm{T}} = \mathbf{U}_m\boldsymbol{\Sigma}_m\mathbf{V}_m^{\mathrm{T}}$, where $\mathbf{U}_m$ and $\mathbf{V}_m$ are the rectangular matrices obtained by retaining the first m columns, and $\boldsymbol{\Sigma}_m$ is the $(m \times m)$ principal minor of $\boldsymbol{\Sigma}$, is the closest rank m matrix to $\mathbf{X}^{\mathrm{T}}$ in the Frobenius norm. To choose the dimension m of the approximate subspace that will contain all the significant information one must look at the singular values, since their value expresses the "signal energy" related to the associated POM. The following examples will show that these values reach a constant plateau, usually called "noise floor", that characterizes the modes which do not contain any significant information. In fact, the use of some form of SVD as a tool to compute the order of a model is a common practice in system identification as well.

If $N \gg n$, then it is more efficient to use the so-called *method of snapshots*. It consists of first computing the matrix $\mathbf{U}$ as the eigenvectors matrix of $\mathbf{X}^{\mathrm{T}}\mathbf{X}$. Once $\mathbf{U}$ is known, since

$$\mathbf{U}^{\mathrm{T}}\mathbf{X}^{\mathrm{T}} = \boldsymbol{\Sigma}\mathbf{V}^{\mathrm{T}},$$

it is clear that the norm of the first m rows of $\boldsymbol{\Sigma}\mathbf{V}^{\mathrm{T}}$ are the singular values, and that these rows, after normalization, are the POMs.

4. Assessing local stability

The proposed method to assess local stability is summarized in the following steps:

(1) Find a periodic orbit. This is usually done by integrating the system for a few periods, possibly with some artificial damping to accelerate convergence to the periodic solution.

(2) Perturb the system and analyze the induced transient to obtain the elements of Eq. (8). When dealing with systems with a large number of degrees-of-freedom the choice of an effective set of perturbations may not be trivial.
(3) Choose a Poincaré section in the phase space and sample the related time histories at periods T to obtain the corresponding Poincaré map.
(4) Analyze the sampled signals, using the snapshot method to compute the POD. The dominant POMs will be selected, based on the relative magnitude of the singular values.
(5) Using the time histories of the POM, obtain a minimal set of signals to be processed. By means of any standard system identification method for multiple output systems [23], e.g. AR based on the least-squares method, an approximate Jacobian matrix is determined, which possesses the dominant eigenvalues of the phenomenon under investigation. The more sophisticated algorithm N4SID [24] can be used for the analysis of experimental data, since it also contains an optimal treatment of noisy signals.
(6) Extract the Floquet multipliers by using any numerical method for the determination of eigenvalues.

Often a prior knowledge of the physical phenomena under investigation will help in choosing the type and level of perturbations. In the extensive experiences of the authors, some of which are reported in the following test cases, no problems were encountered for the selection of correct perturbations. An analysis of the effects of different perturbations and a possible method to choose appropriate signals in complex cases is presented in the test section of this paper. Steps 4 and 5 can be applied recursively to verify the convergence of the solution by increasing the number of samples evaluated. If the problem size is small, step 4 is not necessary. Instead, it becomes nearly mandatory when the dimension of the system is large or when it is necessary to distinguish between physical and spurious eigenvalues, as explained in the following section.

5. Multibody systems and related eigenvalues

The large-scale models that are investigated in this work fall into the class of multidisciplinary multibody systems [6]. They are represented by special DAE systems. To clarify the peculiarities of these models, a brief presentation of the basic formulation is needed.

The motion of a system of rigid/deformable bodies can be described using the principles of classical mechanics. They may lead to a redundant co-ordinate set approach, in which the constraints between inertial bodies are explicitly expressed, or to a minimal co-ordinate set approach where all the constraints are eliminated. The numerical reduction to minimal set equations usually results in methods which are computationally less effective if complicated mechanisms are investigated. The redundant approach instead can be used to easily and automatically generate the equations that model complex systems by means of the multibody formalism. A multibody system can be defined as a collection of bodies in arbitrary motion with respect to each other. These bodies can be connected by algebraic constraints and flexible elements; they can also be subjected to interactional forces that represent other multidisciplinary elements. The advantage of this technique is a simpler formulation, resulting in an easy and versatile implementation, since it is possible to write the free-body dynamics equations for each

body in the global reference frame, with the addition of the constraint equations. One drawback is a larger amount of required degrees-of-freedom, compared to that of the reduced co-ordinate set formulation, which can nonetheless be managed effectively by sparse matrix numerical methods.

The basic equations of motion for the bodies can be described recurring to the Lagrangian multipliers technique to introduce algebraic constraints. Such multipliers are related to the reaction forces exchanged by the bodies, so they are of great significance for engineers. Since their calculation is often required, their direct availability further enhances the overall efficiency of the redundant co-ordinate set against minimal set formulations. The dynamics of the bodies are written in the form of a fully implicit first order differential system by coupling the definition of the momentum, $\boldsymbol{\beta}$, and of the momenta moment, $\boldsymbol{\Gamma}$, of each body to the force and moment equilibrium equations [7]. Given the static moments vector $\mathbf{S}$ and the inertia moments matrix $\mathbf{J}$, the resulting set of equations for each body is

$$\begin{aligned}
&\boldsymbol{\beta} = m\dot{\mathbf{x}} + \boldsymbol{\omega} \times \mathbf{S},\\
&\boldsymbol{\Gamma} = \mathbf{S} \times \dot{\mathbf{x}} + \mathbf{J}\boldsymbol{\omega},\\
&\dot{\boldsymbol{\beta}} = \mathbf{F}(\mathbf{x}, \dot{\mathbf{x}}, \mathbf{R}, \boldsymbol{\omega}, \mathbf{a}, \dot{\mathbf{a}}, \ldots, t) + \mathbf{V}_F,\\
&\dot{\boldsymbol{\Gamma}} + \dot{\mathbf{x}} \times \boldsymbol{\beta} = \mathbf{C}(\mathbf{x}, \dot{\mathbf{x}}, \mathbf{R}, \boldsymbol{\omega}, \mathbf{a}, \dot{\mathbf{a}}, \ldots, t) + \mathbf{V}_C,
\end{aligned} \tag{9}$$

where the forces $\mathbf{F}$ and couples $\mathbf{C}$ may depend on: the configuration represented by the position vector $\mathbf{x}$, the orientation matrix $\mathbf{R}$ and the velocities, translational $\dot{\mathbf{x}}$ and angular $\boldsymbol{\omega}$, the internal states $\mathbf{a}$ that can be generally associated with the multidisciplinary fields that are simultaneously considered; and the time t. The forces $\mathbf{V}_F$ and $\mathbf{V}_C$ are related to the Lagrangian multipliers that represent the actual reaction forces and couples generated by the constraints. Kinematic constraints, both holonomic and non-holonomic, are added as algebraic/differential equations:

$$\begin{aligned}
&\boldsymbol{\Psi}_h(\mathbf{x}, \mathbf{R}, \ldots, t) = 0,\\
&\boldsymbol{\Psi}_{nh}(\mathbf{x}, \dot{\mathbf{x}}, \mathbf{R}, \boldsymbol{\omega}, \ldots, t) = 0,
\end{aligned} \tag{10}$$

The resulting system of non-linear DAE, obtained joining Eqs. (9) and (10), requires a special treatment [25,26] due to the singularity of the algebraic equations if the problem is treated as differential. By calling $\mathbf{y}$ the kinematic unknowns, $\mathbf{z}$ the momentum unknowns and $\boldsymbol{\lambda}$ the algebraic Lagrangian multipliers unknowns, the system can be cast in the following general form

$$\begin{aligned}
&\mathbf{M}(\mathbf{y}, t)\dot{\mathbf{y}} = \mathbf{z},\\
&\dot{\mathbf{z}} = \mathbf{Q}(\mathbf{y}, \dot{\mathbf{y}}, t) - \mathbf{G}^{\mathrm{T}}\boldsymbol{\lambda},\\
&\boldsymbol{\Psi}(\mathbf{y}, t) = \mathbf{0}.
\end{aligned} \tag{11}$$

In these equations, $\mathbf{M}$ is a configuration dependent inertia matrix, $\mathbf{Q}$ are arbitrary external forces and couples and $\mathbf{G} = \mathbf{D}_y\boldsymbol{\Psi}$ is the Jacobian of the holonomic constraints with respect to the kinematic unknowns. The final system is DAE of index three, meaning that three differentiations with respect to time are required to obtain $\dot{\mathbf{y}}$ as a continuous function of $(\mathbf{y}, t)$ [25]. Non-holonomic constraints require a slightly different treatment and result in a lower index DAE system, whose solution is less critical. Numerous techniques have been proposed to solve this kind of problem [25–28]; all the examples presented in the following are solved directly in DAE form

resorting to a fully implicit A/L-stable, second order accurate predictor–corrector integration scheme [7,28].

For index three DAE systems a constraint represents a $(2n-m)$-dimensional manifold

$$\mathscr{M} = \{(\mathbf{y},\mathbf{z}) \,|\, \mathbf{\Psi}(\mathbf{y}) = \mathbf{0},\ \mathbf{D}_y\mathbf{\Psi}(\mathbf{y})\mathbf{M}^{-1}(\mathbf{y})\mathbf{z} = \mathbf{0}\}$$

on which the solution must lie, where n is the dimension of the $\mathbf{y}$ vector, and m is the number of constraint equations $\mathbf{\Psi}(\mathbf{y}) = \mathbf{0}$. The dynamic behaviour of the system represented by Eq. (11) will be locally dominated by the eigenvalues of the linearized vector field that lies in the tangent space of $\mathscr{M}$. To obtain this information one should ideally compute the eigenvalues of the problem stated in terms of the minimal co-ordinate set, which represents the system of differential equations projected on the manifold $\mathscr{M}$. The evaluation of the eigenvalues directly on the DAE systems will result in $(2n-m)$ correct eigenvalues, since m is also the number of Lagrange multipliers, and $2m$ spurious eigenvalues that will not give any useful insight into the dynamics of the mechanism. Consequently, a method to discern among the computed eigenvalues is needed. Usually the m eigenvalues associated to the Lagrangian multipliers assume a minus infinite value, to indicate that the constraint equations are instantaneously satisfied (infinitely fast dynamics). The eigenvalues associated with the redundant co-ordinates instead, assume zero value, since the constrained degrees-of-freedom have no dynamics. So, if the entire spectrum is computed, the significant eigenvalues must be selected in a post-processing phase. However, if only a subset of the eigenvalues is required, an algorithm to select the interesting roots is mandatory. The problems that can be encountered while selecting the significant eigenvalues are illustrated in the following.

5.1. Eigenvalues of a three-masses system

Consider a chain of three masses $m = 1$ shown in Fig. 1. The first and the second mass are connected in series through a spring of stiffness $k = 1$ and a damper with $d = 0.1$. The second and the third mass are rigidly connected. The first mass is constrained to the ground so that the whole system represents a simple oscillator by means of linear DAEs. The resulting equations read:

$$\begin{aligned}
&m\ddot{x}_1 + d\dot{x}_1 - d\dot{x}_2 + kx_1 - kx_2 - \lambda_1 = 0,\\
&m\ddot{x}_2 - d\dot{x}_1 + d\dot{x}_2 - kx_1 + kx_2 - \lambda_2 = 0,\\
&m\ddot{x}_3 + \lambda_2 = 0,\\
&x_1 = 0,\\
&x_2 - x_3 = 0.
\end{aligned} \tag{12}$$

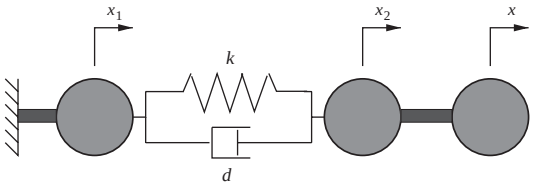

Fig. 1. Three-masses model layout.

Table 1
Eigenvalues computed by means of the implicit matrix approach

Λ	λ
1.000	0.0000
1.000	0.0000
1.000	0.0000
1.000	0.0000
0.9997 + j 7.0665e−4	−0.0250 + j 0.7067
0.9997 − j 7.0665e−4	−0.0250 − j 0.7067
−1.698e−17	−38614
2.600e−22	−49701

Table 2
First four singular values computed for the three-masses problem

σ
6.0745
2.8217
2.2470e − 16
9.2296e − 17

These equations, cast in state space form, yield an eight-dimensional DAE system. Clearly, the same problem can be described in a more compact form by eliminating the constraints

$$2m\ddot{x}_2 + d\dot{x}_2 + kx_2 = 0. \tag{13}$$

Eq. (13) is characterized by the two complex conjugated eigenvalues $\lambda_{1|2} = -0.025 \pm \mathrm{j}\ 0.7067$, that contain all the useful information to be extracted from system (12).

To evaluate these eigenvalues from the DAE system, the method of the implicit matrix proposed by Bauchau and Nikishkov [11] can be used. The eigenvalues of the linearized system matrix λ, and that of the transition matrix $\mathbf{\Phi}(h, 0)$, Λ, are related by

$$\lambda = \frac{1}{h} \ln \Lambda, \tag{14}$$

where h is the time step used to compute the eigenvalues of the transition matrix, and "ln" is the principal natural logarithm. Using a time step of $h = 0.001$ for the present case leads to the eight eigenvalues listed in Table 1.

The correct eigenvalues that represent the dynamics of the system are well approximated, but, as can clearly be seen, they are not the largest modulus ones (it is worth recalling that the eigenvalues on the left, related to the transition matrix, are actually computed). So, seeking the first two eigenvalues with the Arnoldi's method would lead to erroneous information about the stability margin of the system.

The same problem can be solved by applying the method proposed in this paper. In this case the step regarding the sampling process to obtain the Poincaré map is not required since the problem is not periodic. The system is perturbed by giving an initial unit displacement for both the second and third mass. Table 2 lists the amplitude of the first four higher singular values. It clearly shows

Table 3
Eigenvalues computed by means of the POD modes

Λ	λ
0.9997 + j 7.0665e − 4	−0.0250 + j 0.7067
0.9997 − j 7.0665e − 4	−0.0250 − j 0.7067

that there are only two dominant dynamics in the system. A simple least-square fitting of the time histories of the associated POMs gives a Jacobian matrix which possesses the two eigenvalues listed in Table 3. No spurious eigenvalues appear.

6. Numerical tests

The numerical method presented in the previous sections is best illustrated by applying it to two problems. The first example is a classical test case that will also be used to validate the methodology. The second example shows the application of the method to a real multidisciplinary case, a complex helicopter model, including flexible non-linear elements and landing gear components, such as tyres and shock absorbers, are modelled.

6.1. Beam under compressive follower force

A convenient example, useful for the purpose of validating the methodology, is the study of the instability of a simply supported beam under the influence of a periodic compressive follower axial load applied at one of its ends [18]. Consider the continuous beam of length L with mass per unit length m and uniform bending stiffness EJ, subjected to an axial compressive load of the form $P(t) = P_0 + P_1 \cos \omega_P t$, shown in Fig. 2. Call s the co-ordinate along the beam axis and $w(s, t)$ the beam transverse deflection. A distributed linear viscous structural damping d is assumed. The equations of motion can be derived by using Lagrange's formalism. The kinetic energy associated with the transverse beam vibration is

$$T = \int_0^L \frac{1}{2} m \dot{w}(s,t)^2 \, \mathrm{d}s.$$

The potential energy is given by the bending strain energy

$$V = \int_0^L \frac{1}{2} EJ \frac{w''(s,t)^2}{(1 - w'(s,t)^2)} \, \mathrm{d}s.$$

where $(\cdot)' \equiv \partial/\partial s$. Assuming as solution

$$w(s,t) = \sum_i q_i(t) \sin \frac{i\pi s}{L}, \quad i = 1, 2, \ldots, \tag{15}$$

which satisfies all the boundary conditions, it is possible to write the usual Lagrange's equations in terms of the q_i degrees-of-freedom. The generalized forces corresponding to the

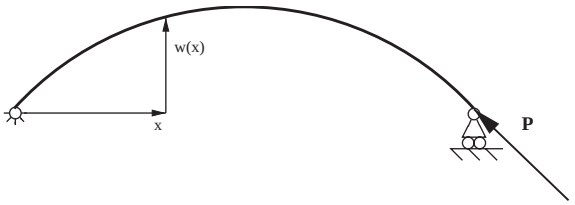

Fig. 2. Simply supported beam under compressive follower load.

follower force $P(t)$ is

$$Q_i = P(t)\frac{\partial}{\partial q_i}\int_0^L \left(\sqrt{1 - w'(s,t)^2} - 1\right) \mathrm{d}s,$$

while the terms associated with the damping forces are equal to

$$D_i = \frac{\partial}{\partial q_i}\int_0^L \mathrm{d}\dot{w}(s,t)\,\mathrm{d}s.$$

The resulting Lagrange's equations are

$$\frac{\mathrm{d}}{\mathrm{d}t}\left(\frac{\partial T}{\partial \dot{q}_i}\right) - \frac{\partial V}{\partial q_i} + D_i = Q_i, \quad i = 1, 2, \ldots . \tag{16}$$

In the non-linear system of equations (16) the different modal degrees-of-freedom are coupled, and each single equation resembles Duffing's equation [5]. The corresponding linearized governing equation is the following:

$$m\ddot{w} + d\dot{w} + EJ\frac{\partial^4 w}{\partial s^4} + (P_0 + P_1\cos\omega_P t)\frac{\partial^2 w}{\partial s^2} = 0. \tag{17}$$

Using the modal expansion of Eq. (15), the PDE above is transformed in a series of Mathieu uncoupled equations for each modal amplitude

$$\ddot{q}_i + \varepsilon\dot{q}_i + \omega_i^2(1 - \mu_i\cos\omega_P t)q_i = 0, \tag{18}$$

where the following parameters are defined

$$\varepsilon = \frac{d}{m}, \quad P_i = \frac{i^2\pi^2 EJ}{L^2}, \quad \omega_i = \frac{i^2\pi^2}{L^2}\sqrt{\frac{EJ}{m}\left(1 - \frac{P_0}{P_i}\right)}, \quad \mu_i = \frac{P_1}{(P_i - P_0)}.$$

It is observed that in many situations the lowest mode is dominant, so that a lumped single mode linearized approximation represents a good simplified model, useful enough to validate stability results.

By considering a solution made of only the first buckling mode of Eq. (15), the stability regions in the μ–Ω plane, $\Omega = \omega_P/2\omega_1$ being a non-dimensional excitation frequency, can be found using the classical Hill's infinite determinant method [29]. A simpler way to obtain the value of the spectral radius for the different conditions is given in Ref. [5], where it is noticed that the determinant of the Jacobian matrix of the Poincaré map associated with Eq. (18) is equal to $\det(DF) = \lambda_1\lambda_2 = \mathrm{e}^{-2\pi\varepsilon/\omega_p}$. If the eigenvalues are complex this product is also equal to the square

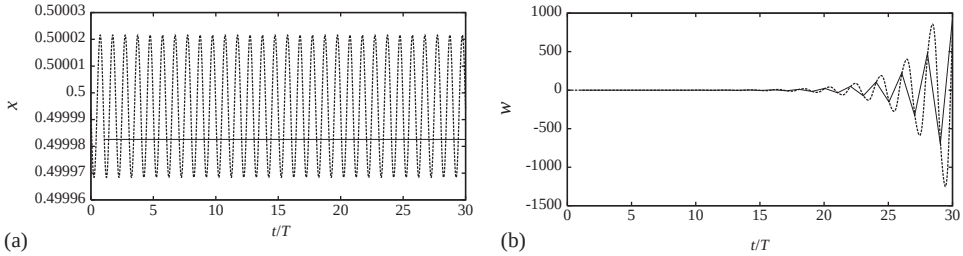

Fig. 3. Unstable periodic motion: $\mu = 0.6$ and $\Omega = 0.9$; - -, time history; —, sampled signal; (a) beam mid-point axial displacement; (b) beam mid-point transversal displacement.

of the spectral radius:

$$\rho = \sqrt{e^{-2\pi\varepsilon/\omega_p}}. \tag{19}$$

In any case the eigenvalues can easily be found by first computing the (2×2) monodromy matrix following the classical approach.

The multibody model built to represent the system under investigation is made of 10 non-linear finite volume three-node beam elements [30]. Such a model includes also the exact representation of the two kinematic constraints, resulting in 264 states. An extremely small static load is applied transversally at the mid-point to model the effect of a beam imperfection. In this case the perturbation load can be easily chosen. It is known that the instability will be related to the first mode, so by applying an impulsive transverse load at the mid-point a perturbation is obtained which possesses a component in the direction of the dominant eigenvector.

Fig. 3 shows two different signals measured for an unstable combination of the parameter μ and Ω; the first one is the axial displacement at the mid-point, while the second is the transverse deflection. It is clear how, if the wrong signals are chosen, the instability may not be tangibly captured. So, an analysis capable of synthesizing all the dominant information from a large model is necessary, especially when it is not clear which is the main instability mechanism. In the latter case the choice of the perturbation signal can be made starting from the identification of the unstable mode running the POD analysis in an unstable condition, while the system is subjected to an impulsive excitation on all of its states. The obtained results will be used in the subsequent tests, where the excitation load will be applied to several antinodes of the first few POMs identified in the instability condition.

After the simulation is run, sampled data are processed to extract the singular values and the POMs. All the sampled time histories of the system states are scaled first, to avoid misleading results in all the cases where mixed physics signals are analyzed together (a situation that can often happen for multidisciplinary models).

Figs. 4 and 5 compare the spectral radius computed from the single mode linear Mathieu model with the results obtained by applying the proposed method to the non-linear multibody model, for two different values of the parameter μ. The data reported on top of the figures show the number of POMs to which the 99.99% of the energy of the time response is associated. Notice how the number of significant modes decreases in the instability areas where the unstable mode dominates the time response.

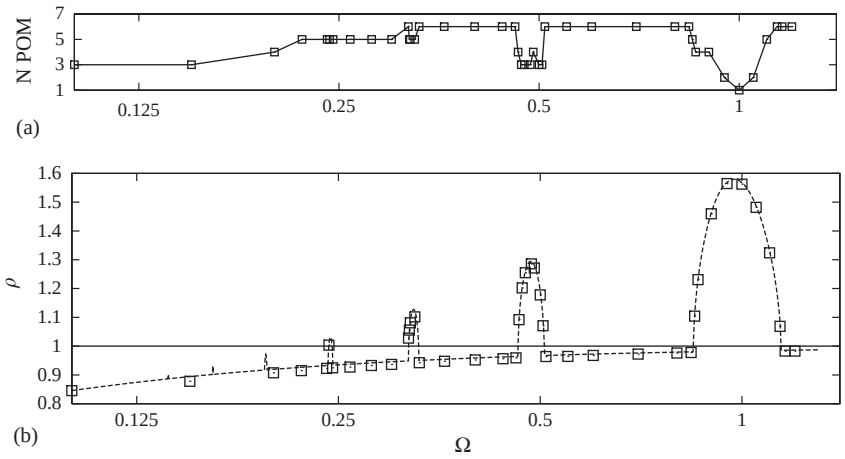

Fig. 4. Comparison of the spectral radius of the monodromy matrix at $\mu = 0.6$ with variable Ω; - -, linear single mode results; □, POD non-linear identification; (a) POD dimensions; (b) spectral radius.

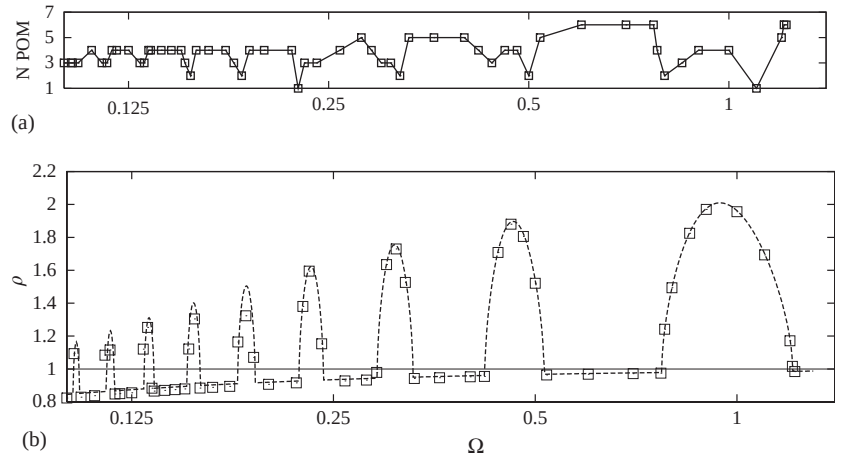

Fig. 5. Comparison of the spectral radius of the monodromy matrix at $\mu = 0.9$ with variable Ω; - -, linear single mode results; □, POD non-linear identification; (a) POD dimensions; (b) spectral radius.

Fig. 6 shows several time histories and phase space projections of the response and the corresponding sampled signal of the beam mid-point transversal displacement, for different values of the parameters. The signals have been scaled to make the diagrams more readable. The agreement between the single mode model and the complete multibody non-linear analysis is very good for stability boundaries computed around the value of $\Omega \simeq 1$, while for low values of Ω the non-linear model gives more damped results. This difference can be explained by looking at the diagrams reported in Fig. 6. For $\Omega = 0.33$–0.842 (Figs. 6e–h), the responses of the system are mainly due to a single mode, as the emerging single turn closed path on the phase space projection shows. Instead, for $\Omega = 0.22$–0.24 (Figs. 6a–d), the responses are characterized by a visible

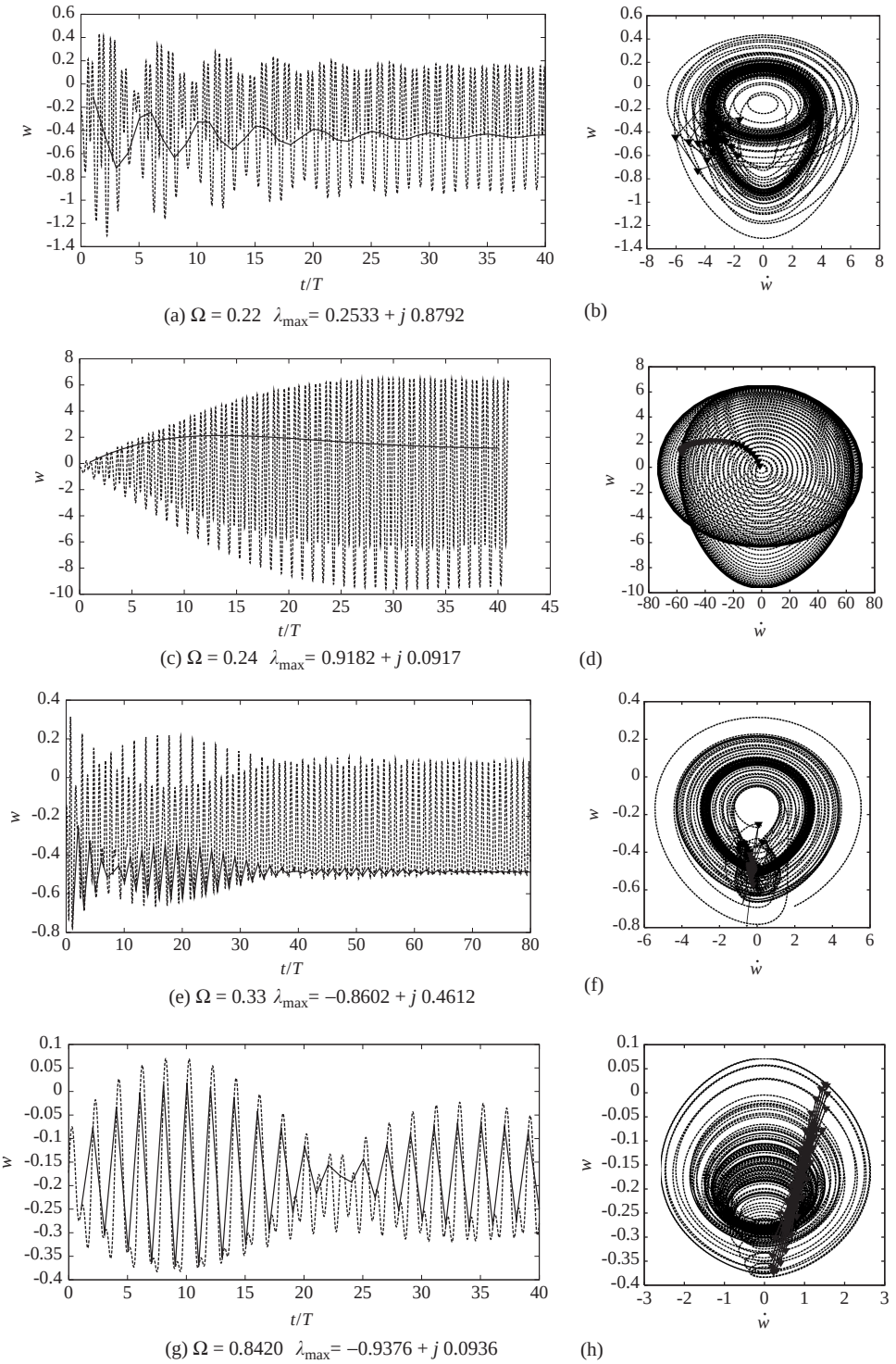

Fig. 6. Stable orbits: transversal displacement w at beam mid-point for different values of Ω; $\mu = 0.6$. On the right phase space projection onto the w–$\dot{w}$ plane; - -, time history; —, sampled signal; ▼, Poincaré map sample.

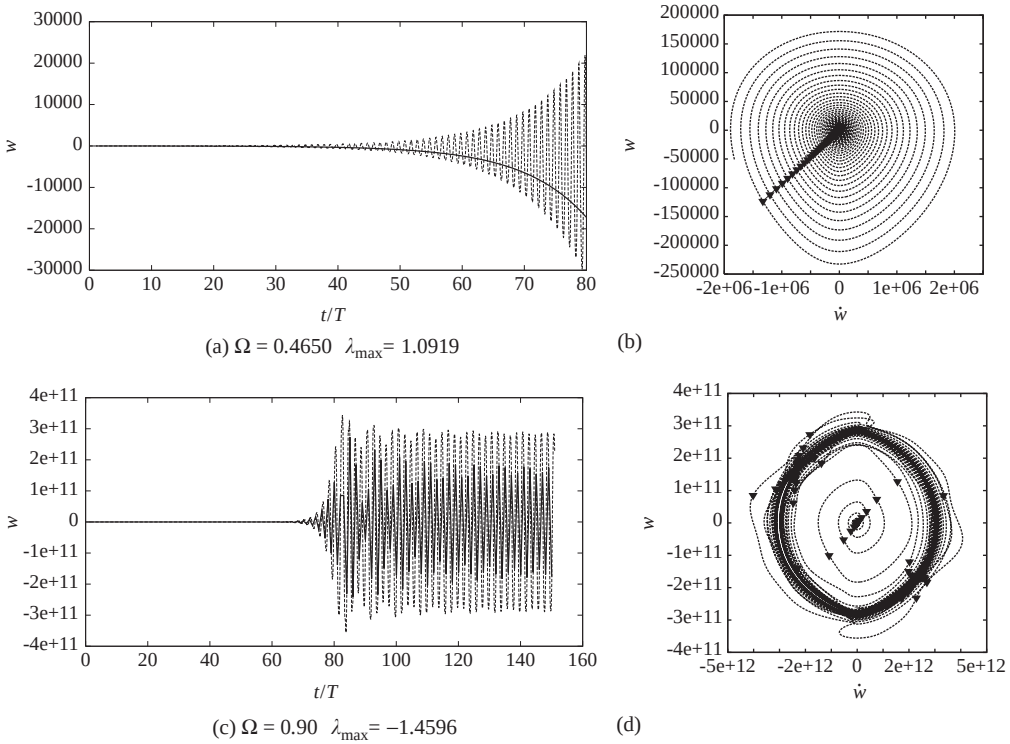

(a) $\Omega = 0.4650$ $\lambda_{max} = 1.0919$ (b)

(c) $\Omega = 0.90$ $\lambda_{max} = -1.4596$ (d)

Fig. 7. Unstable orbits: transversal displacement at beam mid-point for different values of Ω; $\mu = 0.6$. On the right phase space projection onto the w–$\dot{w}$ plane; - -, time history; —, sampled signal; ▼, Poincaré map sample.

activation of the second mode, as the emerging double turn closed path on the phase space projection shows. In the latter cases discrepancies are to be expected since the model cannot be correctly represented by a lumped single mode beam, as in the analytical simplified case.

The Poincaré section of Fig. 7 at $\mu = 0.6$ shows that there are two possible routes to instability. The first is a simple jump bifurcation due to a turning point, while the second drives the system through a period doubling instability. By sampling the same time history with a double period it is possible to evaluate the stability of the new periodic solution. In this case the spectral radius of the single mode linear model will be equal to $\rho = \sqrt{e^{-4\pi\varepsilon/\omega_p}} = 0.9634$. The spectral radius obtained by means of the simulation is equal to $\rho = 0.9411$; in this case 19 POMs are necessary to cover 99.99% of the energy of the time response, consequently the single mode linear model represents only a rough approximation of the more complex non-linear system as captured by the more precise multibody simulation.

Table 4 presents the first three computed eigenvalues for different numbers of time samples processed. It shows how the first one is correctly approximated with 10 samples only, which means that it is sufficient to run a 10-period simulation to correctly identify the dominant λ. For the same problem Bauchau and Nikishkov [12] declare the need for 20 simulation steps to correctly compute the first eigenvalue with the Arnoldi's implicit matrix approach. Considering that, for all the cases when the system is stable, the first significant eigenvalue is not the one with the highest modulus (in this specific case it is the eighth), and that in both cases the most

Table 4
Convergence of eigenvalues for increasing number of samples: $\mu = 0.6,\ \Omega = 0.8$

n		First Eig.		Second Eig.		Third Eig.	
		Value	Error %	Value	Error %	Value	Error %
10	Real	−0.8574	0.27	−0.5943	2.47	0.0393	22.43
	Imag	0.4627	0.22	0.3485	0.91	0.2133	45.20
30	Real	−0.8597	0.00	−0.5858	1.00	0.0347	8.10
	Imag	0.4616	0.02	0.3517	0.00	0.1865	26.96
60	Real	−0.8595	0.02	−0.5844	0.76	0.0342	6.54
	Imag	0.4616	0.02	0.3516	0.03	0.1754	19.40
100	Real	−0.8597	0.00	−0.5800	0.00	0.0321	0.00
	Imag	0.4617	0.00	0.3517	0.00	0.1469	0.00

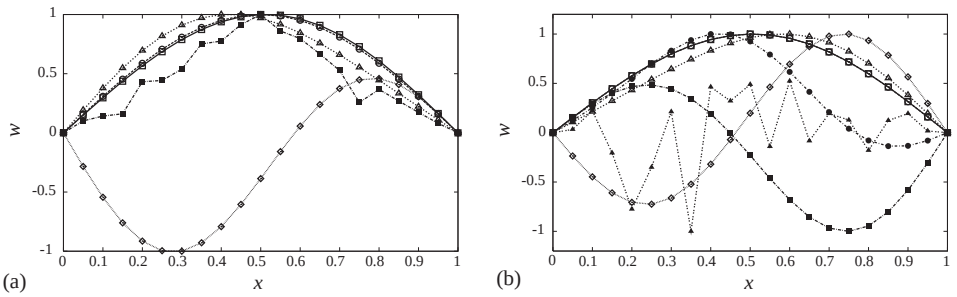

Fig. 8. Computed POM forms for two different parameter sets; (a) $\mu = 0.6\ \Omega = 0.3$; (b) $\mu = 0.9\ \Omega = 0.75$; POMs: □, 1; ◦, 2; △, 3; ◇, 4; ▩, 5; ●, 6; ▲, 7.

computationally intensive phase is the system simulation, the presented method seems to be more effective for these specific multibody applications. Anyway, the efficiency strongly depends on the size of the subspace of unit value eigenvectors related to the number of constraints present in the model.

Fig. 8 shows the POMs computed in two different conditions. The first POM belonging to the "noise floor" is plotted. Its scattered form shows why these modes are negligible. Other perturbations have been tested, all giving correct results, except the case of an axial perturbation applied at the mid-point, because it is represented by a vector tangential to the periodic orbit.

A final test has been conducted using the POM forms computed at $\mu = 0.6$ and $\Omega = 0.3$ (Fig. 8(a)) as a basis to obtain the signals subsequently used for the identifications in different operating conditions. This allows one to save all the operations necessary for the determination of POM forms at the end of each simulation, which may be, for large models, a computationally intensive phase. While the optimality of the POD modal base is lost, for this simple case the small differences do not affect the quality of the results in terms of values of the eigenvalues. These

results cannot be taken as a validation test of a general rule, since there are no great differences between the modal bases computed in different test conditions for this particular problem (Fig. 8). Anyway, it must be noticed that the possibility to use previously computed POM bases, or to partially re-use them, has already been exploited in a completely different field, such as the determination of reduced order model for transonic aerodynamic loads [31]. Further investigations are required to assess the potential of this technique.

6.2. Ground resonance of a helicopter

This example has been chosen to show how this technique can be effectively applied to large and complex models. A brief analysis of the problem will be presented; a more extensive study on this particular phenomenon by means of this novel methodology will be the subject of a future work. The ground resonance is a mechanical instability that may occur when a helicopter stands on the ground [19,32]. The instability is caused by the interaction between the lead-lag in-plane movement of the rotor blades and the dynamics of the rotor supports, in this specific case represented by the aircraft body and its landing gear. In all the articulated helicopter rotors the instability is avoided by using lead-lag dampers on the rotor blades. In this case the periodicity is a result of the rotational movement imposed on the rotor mast, consequently the problem can be treated again as an assessment of stability of a periodically forced non-autonomous system.

The investigation is usually tackled by means of reduced order models in which the structural properties are represented by lumped parameters. The aerodynamic forces of the rotor are usually neglected because they show a limited dependency on the lead-lag motion of the blade. However, this last simplification may not be true since the helicopter rolling and pitching causes a change in blade pitch and the presence of pitch-lag and pitch-flap couplings could affect the rotor aerodynamic loads. To avoid any undue simplification, a detailed multibody model rotorcraft has been built to analyze the ground resonance [33]. By means of the mentioned multibody/multidisciplinary formulation it is possible to represent all the non-linear effects due to large displacements and rotations, aerodynamic loads, non-linear damping and constitutive effects that are usually neglected. The model is representative of a generic medium weight helicopter, and is composed of two main parts: the rotor and the landing gear. For a detailed description of both the reader is referred to Ref. [33]. A short description will be reported here to give an idea of the complexity of the multibody system under investigation. The essential properties of the rotor are detailed in Table 5. The blades are modelled by four parabolic beam elements. The aerodynamic forces are obtained resorting to the classical strip theory, with tabulated aerodynamic coefficients, which account for unsteady flow, uniform inflow and radial flow drag. A dynamic inflow model is considered as well. The blades are attached to the hub by means of elastomeric bearings and a viscoelastic damper. Flexible pitch links and a complete exact kinematic representation of the swashplate are added. The airframe in this case is a single rigid body, even though more complex flexible superelements can easily be added. The tail rotor is instead modelled by a single concentrated force. The three legs of the landing gear are basically modelled by the structural cylinder, the non-linear oleopneumatic shock absorber, the fork, the wheel and the attachment braces, all connected by exact kinematic constraints. The resulting model requires 795 degrees-of-freedom. Analyses made at the nominal angular velocity of 25 rad/s, at different values of the lead-lag damping coefficient are presented. In this case 25 POMs are necessary to obtain a basis

Table 5
Helicopter and rotor properties

Number of blades, n_b	5
Radius, R	8.0 m
Cut-out, R_0	1.66 m
Chord, c	0.5 m
Angular velocity, Ω	25.0 rad/s
Hinge offset, e	0.2 m
Root pitch stiffness, K_θ	10.0 N/rad
Root flap and lag stiffness, K_β, K_ξ	100.0 N/rad
Pitch link stiffness, $M_{c/\theta}$	1.6e5 N m/rad
Blade mass per unit length, m	10.0 Kg/m
Blade inertia per unit length, J_p	1.28 Kg m
Blade twist, θ	-12.0 deg
Twist stiffness, GJ	1.8e6 N m^2
Beam stiffness, EJ_y	1.5e5 N m^2
Chord stiffness, EJ_z	1.0e7 N m^2
Overall mass, M	9500.0 kg
Overall length, L	20.0 m
Roll Inertia, I_x	3000.0 kg m^2
Pitch and Yaw Inertia, I_y, I_z	15000.0 kg m^2

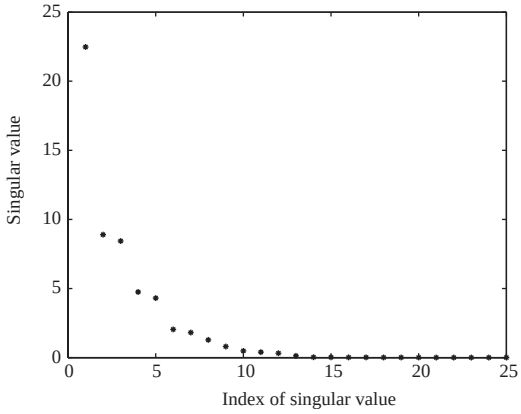

Fig. 9. Singular values for the helicopter model; lead-lag damper coefficient $d = 7e3$ [N m/rad/s].

which covers 99.99% of the energy. Looking at the singular values associated with each POM, shown in Fig. 9, it is clear that the periodic response is dominated by the first 12 eigenvalues.

The periodic orbit is perturbed by means of an impulsive load applied at the tip of blade 1. Fig. 10 shows the identified dominant multipliers. The same multipliers can be transformed by means of Eq. (14) to obtain the eigenvalues of the linearized problem, shown in Fig. 11.

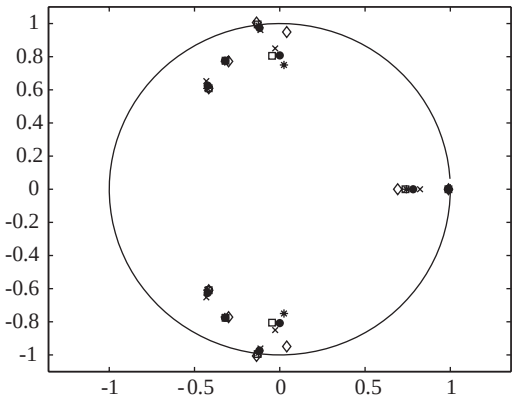

Fig. 10. Floquet multipliers for the helicopter for different lead-lag damper coefficient d values; $\times$, 8.0e3 N m/rad/s; $\bullet$, 7.5e3 N m/rad/s; $*$, 7.0e3 N m/rad/s; $\square$, 6.8 e3 N m/rad/s; $\diamond$, 6.5e3 N m/rad/s.

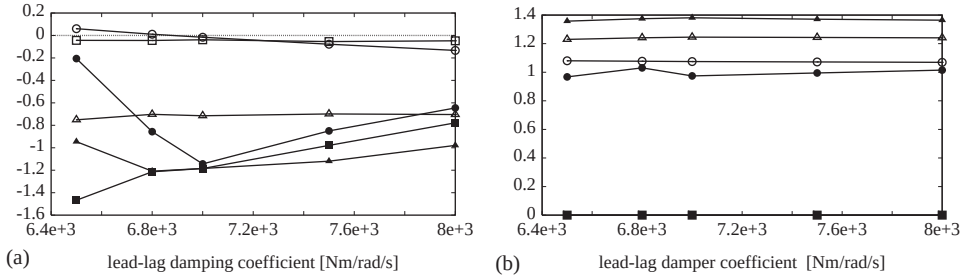

Fig. 11. System eigenvalues obtained transforming the Floquet multipliers; (a) real part; (b) frequency.

The path of the estimated multipliers shows that the system is going through a Naimark–Saker bifurcation, the equivalent for maps of the Hopf bifurcation [5], crossing the value of 6.9e3 N m/rad/s for the lag damper coefficient. The instability is caused by an interaction between the helicopter roll motion, at about 1 Hz, and the retreating lag motion. The resulting orbit followed by the system after the bifurcation belongs to a multi-dimensional two-torus T^2. Since the two frequencies are not simply commensurate, the resulting regime orbit is quasi-periodic, at least from a numerical point of view. Fig. 12 shows two phase space projections of the system orbit before and after the bifurcation. In the first picture it is clear how the system is going toward a fixed point (left bottom corner), as it is expected for a Poincaré map of a periodic orbit. The second instead shows how the Poincaré map seems to form a closed curve made of discrete points, a typical behaviour of a quasi-periodic solution, where the map represents a section of the T^2 torus.

After this first bifurcation the system can still be considered globally stable, since the amplitudes of the resulting oscillations are small. A second bifurcation will lead the system to a major instability that cannot be recovered, as shown in Ref. [33]. However, the stability analysis of the new quasi-periodic orbit is beyond the scope of this work so it is not presented here.

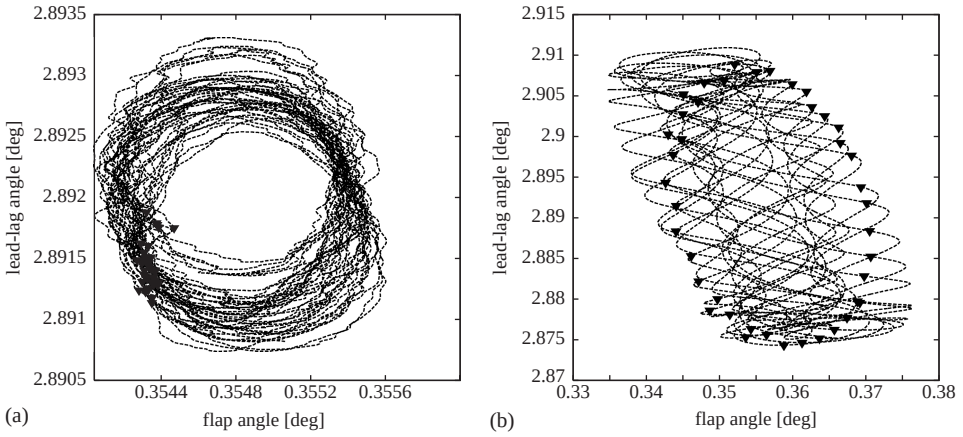

Fig. 12. Phase space projection of the system transient at two different values of lead-lag damping coefficient d: ▼, Poincarè sample; (a) $d = 8e3$ [N m/rad/s] periodic behaviour; (b) $d = 6.5e3$ [N m/rad/s] quasi-periodic behaviour.

7. Concluding remarks

The multibody approach allows the use of modular elements to build a complete system with all the details required for each subpart. In this way it is possible to obtain a model that can be used for different analyses at each development stage, avoiding risky physical oversimplifications. When periodic systems are analyzed, the assessment of their stability boundaries for different sets of operating parameters is often needed before going through any further investigation on the system behaviour. Unfortunately, dealing with such large models, a very high computational burden is required to gain this information by means of classical techniques based on the reconstruction of the entire monodromy matrix. By means of the multibody/multidisciplinary modelling paradigm the designer may deal with a single model useful in a wide range of operating conditions. However, to make this tool really efficient, it must necessarily be coupled to a methodology capable of synthesizing the significant pieces of information in a small set of results.

This paper presented an effective method to overcome these hurdles on the base of a proper orthogonal decomposition. It is shown how, by means of this technique, it is possible to select the dominant dynamics which govern the system response in the form of a small set of combined states/signals. By using classical identification methods, it is straightforward to obtain the dominant Floquet multipliers from these signals. By means of POD it is possible to achieve two additional goals: first of all it gives information about the real dimensions of the subspace on which the dynamic evolution for a particular set of parameters takes place; second, it allows one to rule out all the spurious eigenvalues that may eventually arise when a non-minimal set system of equations is analyzed. The application of the proposed method to the test case of the simply supported beam subjected to an oscillating axial load gave results that have been matched successfully with those that can be obtained for the same problem with more classical methodologies. Few results obtained to assess the ground resonance stability of a large helicopter model show the capabilities of the proposed method in dealing with large multidisciplinary models.

Further tests are required to verify the possibility of adopting a single set of POMs in the identification of the Floquet multipliers for different operating conditions. This set does not need to be the result of a single analysis made at a specific operating condition but can be obtained by merging POMs computed with different parameter values. In fact, if the modal forms are already determined, it will be possible to identify the Floquet multipliers while the simulation is running, stopping it only when a sufficiently accurate result is achieved.

References

[1] G. Sansone, R. Conti, *Non-linear Differential Equations*, Pergamon Press, Oxford, UK, 1964 (translated from the Italian by A. H. Diamond).

[2] A. Lyapunov, *The General Problem of the Stability of Motion*, Princeton University Press, Princeton, NJ, 1947.

[3] T.A. Burton, *Stability and Periodic Solutions of Ordinary and Functional Differential Equations*, Academic Press, Orlando, FL, 1985.

[4] R. Seydel, *Practical Bifurcation and Stability Analysis. From Equilibrium to Chaos*, Springer, New York, 1994.

[5] J. Guckenheimer, P. Holmes, *Nonlinear Oscillations, Dynamical Systems, and Bifurcations of Vector Field*, 3rd Edition, Springer, New York, 1990.

[6] W. Schiehlen, *Multibody Systems Handbook*, Springer, Berlin, 1990.

[7] G. Quaranta, P. Masarati, P. Mantegazza, Multibody analysis of controlled aeroelastic systems on parallel computers, *Multibody Systems Dynamics* 8 (1) (2002) 71–102.

[8] K. Murphy, P. Bayly, L. Virgin, J. Gottwald, Measuring the stability of periodic attractors using perturbation-induced transients: applications to two nonlinear oscillators, *Journal of Sound and Vibration* 172 (1) (1994) 85–102.

[9] H. Matthies, C. Nath, Dynamic stability of periodic solution of large scale nonlinear systems, *Computational Methods in Applied Mechanics and Engineering* 48 (1985) 191–202.

[10] S. Subramanian, G.H. Gaonkar, Parallel fast-floquet analysis of trim and stability for large helicopter models, in: *22nd European Rotorcraft Forum*, Brighton, United Kingdom, September 17–19, 1996, pp. 94.1–94.14.

[11] O.A. Bauchau, Y.G. Nikishkov, An implicit transition matrix approach to stability analysis of flexible multi-body systems, *Multibody Systems Dynamics* 5 (3) (2001) 279–301.

[12] O.A. Bauchau, Y.G. Nikishkov, An implicit floquet analysis for rotorcraft stability evaluation, *Journal of the American Helicopter Society* 46 (2001) 200–209.

[13] P. Holmes, J. Lumley, G. Berkooz, *Turbulence, Coherent Structures, Dynamical Systems and Symmetry*, Cambridge University Press, Cambridge, 1996.

[14] B. Epureanu, E. Dowell, K. Hall, Reduced-order models of unsteady viscous flows in turbomachinery using viscous-inviscid coupling, *Journal of Fluids and Structures* 15 (2001) 255–273.

[15] B. Feeny, R. Kappagantu, On the physical interpretation of proper orthogonal modes in vibrations, *Journal of Sound and Vibration* 211 (4) (1998) 607–616.

[16] M. Azeez, A. Vakakis, Proper orthogonal decomposition (POD) of a class of vibroimpact oscillations, *Journal of Sound and Vibration* 240 (5) (2001) 859–889.

[17] R. Ruotolo, C. Surace, Using SVD to detect damage in structures with different operational conditions, *Journal of Sound and Vibration* 226 (3) (1999) 425–439.

[18] V.V. Bolotin, *Nonconservative Problems of the Theory of Elastic Stability*, Pergamon Press, Oxford, 1963.

[19] R.P. Coleman, A.M. Feingold, Theory of self-excited mechanical oscillations of helicopter rotors with hinged blades, REPORT 1351, NACA, 1958.

[20] P. Friedmann, C. Hammond, T.-H. Woo, Efficient numerical treatment of periodic systems with application to stability problems, *International Journal for Numerical Methods in Engineering* 11 (1977) 1117–1136.

[21] G.H. Golub, C.F. van Loan, *Matrix Computation*, 2nd Edition, The John Hopkins University Press, Baltimore, 1991.

[22] Y. Saad, *Iterative Methods for Sparse Linear Systems*, PWS Publishing Company, Boston, MA, 1996.

[23] L. Lijung, *System Identification—Theory for the User*, 2nd Edition, Prentice-Hall, Upper Saddle River, NJ, 1999.

[24] P. Van Overschee, B. De Moor, N4SID: subspace algorithms for the identification of combined deterministic–stochastic systems, *Automatica* 30 (1) (1994) 75–93.
[25] K.E. Brenan, S.L.V. Campbell, L.R. Petzold, *Numerical Solution of Initial-Value Problems in Differential-Algebraic Equations*, North-Holland, New York, 1989.
[26] E. Hairer, G. Wanner, *Solving Ordinary Differential Equations II. Stiff and Differential Algebraic Problems*, 2nd revised edition, Springer, Berlin, 1996.
[27] C.L. Bottasso, M. Borri, L. Trainelli, Integration of elastic multibody systems by invariant conserving dissipating algorithms. II. Numerical schemes and applications, *Computer Methods in Applied Mechanics and Engineering* 190 (2001) 3701–3733.
[28] P. Masarati, M. Lanz, P. Mantegazza, Multistep integration of ordinary, stiff and differential-algebraic problems for multibody dynamics applications, in: XVI Congresso Nazionale AIDAA, Palermo, 24–28 Settembre, 2001.
[29] P. Hagedorn, *Non-Linear Oscillations*, Clarendon Press, Oxford, UK, 1981.
[30] G.L. Ghiringhelli, P. Masarati, P. Mantegazza, A multi-body implementation of finite volume beams, *American Institute of Aeronautics and Astronautics Journal* 38 (2000) 131–138.
[31] J.P. Thomas, E.H. Dowell, K.C. Hall, Three-dimensional transonic aeroelasticity using proper orthogonal decomposition based reduced order models, in: *Proceedings of the 42nd AIAA/ASME/ASCE/AHS/ASC Structures, Structural Dynamics, and Materials Conference and Exhibit*, Seattle, WA, 16–19 April 2001.
[32] R.L. Bielawa, *Rotary Wing Structural Dynamics and Aeroelasticity*, AIAA, Washington, DC, 1992.
[33] S. Gualdi, P. Masarati, M. Morandini, G.L. Ghiringhelli, A multibody approach to the analysis of helicopter-terrain interaction, in: *28th European Rotorcraft Forum*, Bristol, UK, 2002.